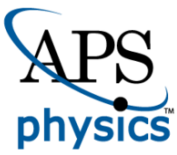

Superfluid Weight Bounds from Symmetry and Quantum Geometry in Flat Bands

Jonah Herzog-Arbeitman, Valerio Peri, Frank Schindler, Sebastian D. Huber, and B. Andrei Bernevig

Phys. Rev. Lett. **128**, 087002 — Published 25 February 2022

DOI: 10.1103/PhysRevLett.128.087002

Superfluid Weight Bounds from Symmetry and Quantum Geometry in Flat Bands

Jonah Herzog-Arbeitman,[1] Valerio Peri,[2] Frank Schindler,[3] Sebastian D. Huber,[2] and B. Andrei Bernevig[1, 4, 5]

[1]*Department of Physics, Princeton University, Princeton, NJ 08544*
[2]*Institute for Theoretical Physics, ETH Zurich, 8093 Zürich, Switzerland*
[3]*Princeton Center for Theoretical Science, Princeton University, Princeton, NJ 08544, USA*
[4]*Donostia International Physics Center, P. Manuel de Lardizabal 4, 20018 Donostia-San Sebastian, Spain*
[5]*IKERBASQUE, Basque Foundation for Science, Bilbao, Spain*

(Dated: February 4, 2022)

Flat-band superconductivity has theoretically demonstrated the importance of band topology to correlated phases. In two dimensions, the superfluid weight, which determines the critical temperature through the Berezinksii-Kosterlitz-Thouless criteria, is bounded by the Fubini-Study metric at zero temperature. We show this bound is nonzero within flat bands whose Wannier centers are obstructed from the atoms — even when they have identically zero Berry curvature. Next, we derive general lower bounds for the superfluid weight in terms of momentum space irreps in all 2D space groups, extending the reach of topological quantum chemistry to superconducting states. We find that the bounds can be naturally expressed using the formalism of real space invariants (RSIs) that highlight the separation between electronic and atomic degrees of freedom. Finally, using exact Monte Carlo simulations on a model with perfectly flat bands and strictly local obstructed Wannier functions, we find that an attractive Hubbard interaction results in superconductivity as predicted by the RSI bound beyond mean-field. Hence, obstructed bands are distinguished from trivial bands in the presence of interactions by the nonzero lower bound imposed on their superfluid weight.

Introduction. In a topological insulator, the ground state Wannier functions face an obstruction to exponential localization[1–5]. This real-space picture connects bulk topological invariants computed from the bands in momentum space to the local chemistry of electronic states. Topological states can be either stable or fragile, and are classified by their symmetry properties in momentum space[6–9]. Fragile states can be trivialized by mixing with non-topological bands[10–12], while stable states cannot. Moreover, stable topological phases are distinguished by their gapless edge states[13,14], while fragile phases have anomalous boundary signatures exposed by twisted boundary conditions[15,16], magnetic flux[17], or defects[18]. Although our understanding of non-interacting topological bands is nearly exhaustive,[19–22], this is not the case for interactions within topological bands.

Superconductivity in topological bands[23,24] is of interest since its discovery within the fragile flat bands[25–34] of twisted bilayer graphene[35–41]. Discovered in Ref. 42, superconducting order in flat bands, specifically the superfluid weight, originates from quantum geometry characterized by the Fubini-Study metric and has gathered much excitement[43–49]. The quantum metric, though distinct from the band topology, is bounded by the Chern or (Euler) winding numbers[23,50,51]. These early results suggest that topological quantum chemistry could provide general lower bounds, making contact with materials databases[52–54]. Our work affirms this suggestion, yielding nonzero bounds in phases without winding numbers. Our bounds are given by another quantized number, the real space invariant (RSI)[15], which uses symmetries to characterize topological, obstructed Wannier centers (OWCs), and trivial bands.

From a materials perspective, although topological bands are abundant within real crystals, a significant portion are topologically trivial at the Fermi level. Topologically trivial bands with space group symmetries have a finer classification which divides them into trivial atomic bands, where electrons are exponentially localized at the atomic sites, and bands with OWCs which, while exponentially localized, are necessarily centered off the atoms[55–57]. Remarkably, we show that, like topological bands, OWCs have a nonzero, lower-bounded Fubini-Study metric even without Berry curvature[58,59]. When flat OWC bands are partially filled under attractive interactions, they possess a superconducting instability.

The zero-temperature superfluid weight $[D_s]_{ij}$ of an isolated flat band within BCS theory[59] is[60]

$$[D_s]_{ij} = 2|\Delta|\sqrt{\nu(1-\nu)}\int \frac{d^2k}{(2\pi)^2} g_{ij}(\mathbf{k}) \tag{1}$$

where Δ is the superconducting gap, ν is the filling fraction of the flat bands, $\mathbf{k}$ is a momentum in the Brillouin zone (BZ) with area $(2\pi)^2/\Omega_c$ (Ω_c is the unit cell area), and g_{ij} is the Fubini-Study quantum metric. A nonzero superfluid weight implies a finite critical superconducting temperature[61,62] and a supercurrent $\mathbf{J} = -4D_s\mathbf{A}$, where $\mathbf{A}$ is the vector potential in the London gauge. In a Hamiltonian with N_{orb} orbitals and N_{occ} occupied bands, we define the (abelian) quantum geometric tensor[63]

$$\text{Tr } \mathcal{G}_{ij} = \text{Tr } P\partial_i P\partial_j P = g_{ij} + \frac{i}{2}f_{ij}, \tag{2}$$

where $P(\mathbf{k})$ is the $N_{\text{orb}} \times N_{\text{orb}}$ gauge-invariant projection matrix onto the occupied bands, ∂_i is a momentum-space derivative, and the trace is over the matrix indices. The abelian Berry curvature $f_{ij} = -f_{ji}$ is well studied while the positive semi-definite quantum metric $g_{ij} = g_{ji}$ is an object of more recent interest[63–83]. With spatial rotation

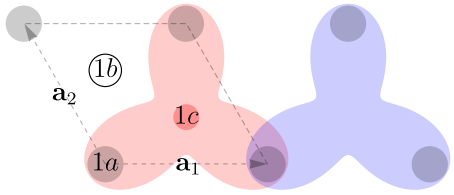

FIG. 1. Wannier basis at 1c $= \frac{2}{3}\mathbf{a}_1 + \frac{1}{3}\mathbf{a}_2$. The Wannier state $|A_{1c}\rangle$ (red) centered at 1c is supported only on the neighboring atomic sites (grey) with $A, {}^1E$, and ${}^2E$ orbitals. Only one site overlaps with neighboring Wannier states (blue).

symmetry, $[D_s]_{ij}$ is determined by the trace of g_{ij}[84]

$$G = \frac{1}{2}\int \frac{d^2k}{(2\pi)^2} \mathrm{Tr}\, \boldsymbol{\nabla} P \cdot \boldsymbol{\nabla} P \geq 0, \tag{3}$$

which is coordinate invariant, dimensionless, and importantly is quadratic in $P(\mathbf{k})$[60]. We give an efficient numerical discretization formula in Ref. 60.

Flat Band Model. We begin by constructing an OWC model in the space group $p3$ generated by spinless C_3 symmetry and translations along the lattice vectors $\mathbf{a}_1 = (1,0), \mathbf{a}_2 = C_3\mathbf{a}_1$. At the origin (the 1a position), we place electrons in the $A, {}^1E, {}^2E$ irreps. These orbitals induce band representations[85,86] with irreps defined by

$$\begin{aligned} A_{1a} \uparrow p3 &= \Gamma_1 + K_1 + K_1', \quad C_3 = +1 \\ {}^1E_{1a} \uparrow p3 &= \Gamma_2 + K_2 + K_3', \quad C_3 = e^{-\frac{2\pi i}{3}} \\ {}^2E_{1a} \uparrow p3 &= \Gamma_3 + K_3 + K_2', \quad C_3 = e^{\frac{2\pi i}{3}} \end{aligned} \tag{4}$$

where $\Gamma = (0,0)^{\mathrm{T}}, K = \frac{2\pi}{3}(\mathbf{b}_1 + \mathbf{b}_2), K' = -\frac{2\pi}{3}(\mathbf{b}_1 + \mathbf{b}_2)$ are the high symmetry points, and $\mathbf{a}_i \cdot \mathbf{b}_j = \delta_{ij}$. The full group theory data can be found on the Bilbao Crystallographic server[87–89]. To construct a flat band OWC from these orbitals, we will use a Wannier basis centered at the 1c position *off* the atomic sites at 1a as in Fig. 1. We form the Wannier states

$$|\mathbf{R}, A_{1c}\rangle = \frac{1}{3} T_{\mathbf{R}} \sum_{j=0}^{2} \tilde{C}_3^j (|0,A\rangle + |0,{}^1E\rangle + |0,{}^2E\rangle), \tag{5}$$

where $T_{\mathbf{R}}$ is the translation operator by $\mathbf{R}$, $\tilde{C}_3$ is the rotation operator about the 1c position, and $|0,\rho\rangle$ are the ρ orbitals in unit cell 0. Taking $\tilde{C}_3 \to e^{\mp\frac{2\pi i}{3}}\tilde{C}_3$ in Eq. (5) yields ${}^1E$ and ${}^2E$ states at 1c. It is easy to check that the states $|\mathbf{R}, A_{1c}\rangle$ are orthonormal: $\langle \mathbf{R}, A_{1c}|\mathbf{R}', A_{1c}\rangle$ is nonzero only if $\mathbf{R}$ and $\mathbf{R}'$ are nearest neighbors, and in this case the only overlap is on a single site which vanishes due to $\tilde{C}_3$ eigenvalues of the orbitals. Fourier transforming Eq. (5) to obtain the eigenstate $|\mathbf{k}, A_{1c}\rangle$ yields the eigenvector $U_\alpha(\mathbf{k}) = \langle \mathbf{k}, \alpha | \mathbf{k}, A_{1c}\rangle$, $\alpha = A, {}^1E, {}^2E$:

$$U(\mathbf{k}) = \frac{1}{3}\begin{pmatrix}1\\1\\1\end{pmatrix} + \frac{1}{3}\begin{pmatrix}1\\ e^{\frac{4\pi i}{3}}\\ e^{\frac{2\pi i}{3}}\end{pmatrix} e^{i\mathbf{k}\cdot(\mathbf{a}_1+\mathbf{a}_2)} + \frac{1}{3}\begin{pmatrix}1\\ e^{\frac{2\pi i}{3}}\\ e^{\frac{4\pi i}{3}}\end{pmatrix} e^{i\mathbf{k}\cdot\mathbf{a}_2}, \tag{6}$$

and the local momentum-space Hamiltonian

$$h(\mathbf{k}) = -|t| U(\mathbf{k}) U^\dagger(\mathbf{k}) \equiv -|t| P(\mathbf{k}) \tag{7}$$

which has three exactly flat bands: the A_{1c} band at energy $-|t|$ and the degenerate ${}^1E_{1c}$ and ${}^2E_{1c}$ bands at zero energy. At filling 1/3, $h(\mathbf{k})$ has the band representation

$$\Gamma_1 + K_3 + K_3' = A_{1c} \uparrow p3, \tag{8}$$

confirming our construction in real space. We also calculate the Berry connection in crystalline coordinates,

$$A_i(\mathbf{k}) = U^\dagger(\mathbf{k}) i\partial_i U(\mathbf{k}) = (-1/3, -2/3)_i\,, \tag{9}$$

which is the expectation value of the lattice position operator in the occupied bands. Noting that the lattice position operator is only defined mod 1, Eq. (9) confirms that the states are located at the 1c position. Because $A_i(\mathbf{k})$ is independent of $\mathbf{k}$ (up to a gauge choice), the Wilson loop bands are perfectly flat[90] and the Berry curvature is identically zero. Topologically, the model is therefore trivial. However, we calculate the quantum metric in cartesian coordinates (a is the lattice constant):

$$g_{ij}(\mathbf{k}) = \frac{1}{2}\mathrm{Tr}\, \partial_i P(\mathbf{k}) \partial_j P(\mathbf{k}) = a^2\delta_{ij}/6, \tag{10}$$

so the mean-field superfluid weight in Eq. (1) is nonzero despite the model being topologically trivial and having compact Wannier functions (zero correlation length)[57].

It is natural to ask what indices describe these compact OWC phases. By definition, they are induced by off-site atomic orbitals, so topological quantum chemistry can identify them because their symmetry data does not match any of the orbitals present in the lattice. This is different than the stable and fragile indices which are independent of the basis orbitals.

Wilson loops can also identify OWCs. A useful reference is the SSH chain[91] where an eigenvalue of π of the Wilson loop operator identifies the off-site states[92,93]. Lastly, OWCs can be most naturally defined using the RSI formalism developed in Ref. 15. RSIs are local quantum numbers which are well-defined in fragile and OWC phases where they supply lower bounds on the number of states at the high symmetry Wyckoff positions. By definition, RSIs are invariant under symmetry-preserving adiabatic deformations. Since the Wannier states in OWCs cannot be moved to atomic sites without closing a gap, they are characterized by a nonzero RSI off an atomic site. In space group $p3$, the RSIs at a C_3-symmetric Wyckoff positions are

$$\delta_1 = m({}^1E) - m(A), \quad \delta_2 = m({}^2E) - m(A) \tag{11}$$

and $m(\rho)$ is the number of ρ irreps. The RSIs can be conveniently calculated from the momentum space symmetry data[15]. In our model, the only nonzero RSIs are off the atomic sites at the 1c position, $(\delta_{1c,1}, \delta_{1c,2}) = (-1,-1)$. We will now show that, in generality, these off-site RSIs are responsible for a bounded superfluid weight.

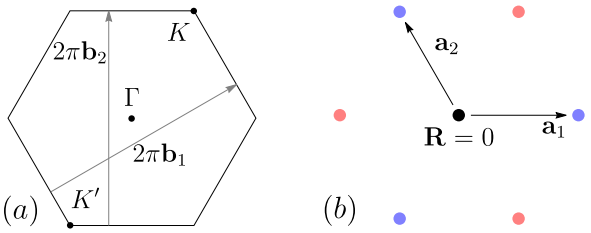

FIG. 2. C_3 Bounds. (a) We label the C_3-invariant points Γ, K, and K' in the BZ. (b) By taking linear combinations of $P(\mathbf{k})$, we find lower bounds for the harmonics at $|\mathbf{R}| = 1$, shown in red and blue. Higher harmonics are not shown.

Lower Bounds in Real Space. We derive general lower bounds for the superfluid weight in terms of RSIs and orbital positions to show that nonzero superfluid weight is a generic feature of partially filled OWC bands, as has been shown for Chern insulators and Euler insulators[23,50]. Our bounds also apply to all 2D topological bands[60] including fragile bands. Here, for simplicity, we prove a lower bound for our model with C_3 and all orbitals at the 1a position. Our starting point is a real space expression for $P(\mathbf{k})$, the projector onto the occupied A_{1c} band. If all orbitals are at the 1a position, then $h(\mathbf{k})$ and $P(\mathbf{k})$ are periodic under $\mathbf{k} \to \mathbf{k} + 2\pi\mathbf{b}_i$. Thus there is a Fourier representation

$$P(\mathbf{k}) = \sum_{\mathbf{R}} e^{-i\mathbf{R}\cdot\mathbf{k}} p(\mathbf{R}), \;\; p(\mathbf{R}) = \int \frac{dk^1 dk^2}{(2\pi)^2} e^{i\mathbf{R}\cdot\mathbf{k}} P(\mathbf{k}), \tag{12}$$

defined in terms of the harmonics $p(\mathbf{R})$, which are $N_{\text{orb}} \times N_{\text{orb}}$ matrices, the lattice vectors $\mathbf{R}$, and the dimensionless crystal momenta k^i. Note that $P(\mathbf{k})$ is the momentum space Green's function[94], so $p(\mathbf{R})$ is the real space correlation function. The harmonics obey a normalization condition

$$\sum_{\mathbf{R}} ||p(\mathbf{R})||^2 = \int \frac{dk^1 dk^2}{(2\pi)^2} \text{Tr } P(\mathbf{k}) = N_{\text{occ}} = 1, \tag{13}$$

where $||A||^2 = \text{Tr } A^\dagger A$ is the squared Frobenius norm[60]. Rewriting Eq. (3) in real space, we find

$$G = \frac{1}{2} \int \frac{d^2k}{(2\pi)^2} \text{Tr } \boldsymbol{\nabla} P \cdot \boldsymbol{\nabla} P = \frac{1}{2\Omega_c} \sum_{\mathbf{R}} |\mathbf{R}|^2 ||p(\mathbf{R})||^2 \; . \tag{14}$$

We will use symmetry eigenvalues to show that $||p(\mathbf{a}_1)||$ and symmetry-related terms are bounded below. This immediately gives a bound for G because $G \geq \frac{1}{2\Omega_c}|\mathbf{a}_1|^2||p(\mathbf{a}_1)||^2$ since all terms in Eq. (14) are positive semi-definite. Indeed, all are *positive* definite except for the zero mode $p(0)$, the constant mode of $P(\mathbf{k})$.

The momentum space irreps consist of the C_3 eigenvalues in the occupied bands at Γ, K, K' (see Fig. 2a). The irrep multiplicities $m(\rho)$ obey[60]

$$m(\Gamma_1) + e^{\frac{2\pi i}{3}} m(\Gamma_2) + e^{-\frac{2\pi i}{3}} m(\Gamma_3) = \text{Tr } D[C_3] P(\Gamma), \tag{15}$$

and similarly for K and K'. Here $D[C_3] = \text{diag}(1, e^{-\frac{2\pi i}{3}}, e^{\frac{2\pi i}{3}})$ is the representation matrix of C_3 on the orbitals. Thus the irrep multiplicities give information about $P(\mathbf{k})$. Writing out and summing Eq. (12) at each high-symmetry momentum gives

$$P(\Gamma) + e^{\frac{2\pi i}{3}} P(K) + e^{\frac{4\pi i}{3}} P(K') = 3 \sum_{n=1}^{3} p(-C_3^n \mathbf{a}_1) + \ldots, \tag{16}$$

where the dots represent higher harmonics $p(\mathbf{R})$ for $|\mathbf{R}| > |\mathbf{a}_i|$ (see Fig. 2b). Crucially, the roots of unity cancel $p(0)$, so only harmonics at $\mathbf{R} \neq 0$ appear in Eq. (16). We now bound Eq. (16) on both sides. To manipulate the momentum space side, we use an elementary inequality[95]

$$||A||^2 \geq |\text{Tr } SA|^2 / \text{Rk}(A) \quad \forall S \text{ unitary}, \tag{17}$$

proven in Ref. 60. Choosing $A = P(\Gamma) + e^{\frac{2\pi i}{3}} P(K) + e^{-\frac{2\pi i}{3}} P(K')$, we see $1/\text{Rk}(A) \geq 1/3$ because A is a 3×3 matrix, and with $S = D[C_3]$, we find with Eq. (15):

$$\begin{aligned} |\text{Tr } SA|^2 &= \frac{9}{4}(m(K_3) + m(K_3') - m(\Gamma_2) - m(\Gamma_3))^2 + \\ &\frac{3}{4}(m(\Gamma_2) - m(\Gamma_3) + m(K_1) - m(K_2) - m(K_1') + m(K_2'))^2 \\ &= 9(\delta_{1c,1}^2 - \delta_{1c,1}\delta_{1c,2} + \delta_{1c,2}^2), \end{aligned} \tag{18}$$

where we first used Eq. (15) to write the trace in terms of momentum space irreps, and then used the tables in Ref. 15 to rewrite them in terms of the RSIs in Eq. (11).

Taking the Frobenius norm of Eq. (16) and applying the triangle inequality to the real space side gives

$$||A|| \leq 3(||p(\mathbf{a}_1)|| + ||p(C_3\mathbf{a}_1)|| + ||p(C_3^2\mathbf{a}_1)|| + \ldots), \tag{19}$$

where the dots are higher harmonics and we used $||p(\mathbf{R})|| = ||p(-\mathbf{R})||$ which follows from Eq. (12). We check explicitly that Eq. (19) is not a tight inequality (by a factor of 3) and prevents our bound from being saturated by this model. All other inequalities are tight.

We next use C_3 symmetry which ensures $||p(\mathbf{R})|| = ||p(C_3\mathbf{R})||$[60]. Because we have a lower bound for $||A||^2$, Eq. (19) proves that $||p(\mathbf{R})|| \neq 0$ for some $\mathbf{R} \neq 0$. We now employ an optimization argument:

$$\frac{1}{2\Omega_c} \sum_{\mathbf{R}} |\mathbf{R}|^2 ||p(\mathbf{R})||^2 \geq \min_{\psi_{\mathbf{R}}} \frac{1}{2\Omega_c} \sum_{\mathbf{R}} |\mathbf{R}|^2 |\psi_{\mathbf{R}}|^2, \tag{20}$$

where the minimization is taken over all $\psi_{\mathbf{R}} \in \mathbb{R}$ obeying

$$\sum_{\mathbf{R}} |\psi_{\mathbf{R}}|^2 = 1, \;\; |\psi_{\mathbf{R}}| = |\psi_{-\mathbf{R}}|, \;\; ||A|| = 9|\psi_{\mathbf{a}_1}| + \ldots, \tag{21}$$

and the dots denote terms depending on $\psi_{|\mathbf{R}|>|\mathbf{a}_1|}$. As such, the space of admissible $|\psi_{\mathbf{R}}|$ described by Eq. (21) includes the choice where $|\psi_{\mathbf{R}}| = ||p(\mathbf{R})||$. By keeping only the constraints in Eq. (21), and not the restriction that $\psi_{\mathbf{R}}$ be the Fourier transform of a projection matrix, we can perform the minimization in Eq. (20) directly.

A lemma we prove in Ref. 60 shows that the minimum occurs when $||A|| = 9|\psi_{\mathbf{a}_1}|$, i.e., when Eq. (19) is saturated with the lowest harmonics possible. This is expected because higher harmonics have larger $|\mathbf{R}|^2$ weights. Adding up the contributions from the inner six harmonics $||p(\mathbf{R})||^2$ in Fig. 2, we find[60]

$$\frac{1}{2\Omega_c}\sum_{\mathbf{R}}|\mathbf{R}|^2||p(\mathbf{R})||^2 \geq \frac{a^2}{9\Omega_c}(\delta_{1c,1}^2 - \delta_{1c,1}\delta_{1c,2} + \delta_{1c,2}^2)\ . \tag{22}$$

Plugging in $\delta_{1c,1} = \delta_{1c,2} = -1$ from Eq. (11), we obtain $G \geq a^2/9\Omega_c = 2/9\sqrt{3}$, a factor of 3 below the exact calculation in Eq. (10). The RSIs in Eq. (22) show that states off the atomic positions (1a in this case), which define OWCs, enforce a nonzero superfluid weight. We obtain bounds for all 2D space groups in Ref. 60.

Hubbard Model. We have shown that single-particle OWCs and fragile states have a nonzero superfluid weight at $T = 0$. However, $[D_s]_{ij}$ in Eq. (1) is obtained from mean-field BCS theory, which may seem unsuitable to treat flat band systems lacking a well-defined Fermi surface. We resort to exact numerical simulations to check its validity at finite temperature.

Using the Hamiltonian $h(\mathbf{k})$ defined in Eq. 7, we form a spinful Hamiltonian with $h_\uparrow(\mathbf{k}) = h(\mathbf{k})$ and $h_\downarrow(\mathbf{k}) = \mathcal{T}h_\uparrow(\mathbf{k})\mathcal{T}^{-1} = h^*(-\mathbf{k})$ which preserves time-reversal $\mathcal{T}$. Here $\uparrow,\downarrow$ label the spins. Including an attractive Hubbard term with strength $|U|$, the full Hamiltonian is

$$H = -|t|\sum_{\mathbf{R},\sigma} w^\dagger_{\mathbf{R}\sigma}w_{\mathbf{R}\sigma} - |U|\sum_{\mathbf{R}\alpha} c^\dagger_{\mathbf{R}\alpha\uparrow}c^\dagger_{\mathbf{R}\alpha\downarrow}c_{\mathbf{R}\alpha\downarrow}c_{\mathbf{R}\alpha\uparrow}, \tag{23}$$

where $w^\dagger_{\mathbf{R}\uparrow}$ creates the Wannier state in Eq. (5), $w^\dagger_{\mathbf{R}\downarrow} = \mathcal{T}w^\dagger_{\mathbf{R},\uparrow}\mathcal{T}^{-1}$, $c^\dagger_{\mathbf{R}\alpha\sigma}$ is the creation operator in unit cell $\mathbf{R}$, orbital α, and spin $\sigma = \{\uparrow,\downarrow\}$. The attractive Hubbard model does not suffer from the fermionic sign problem, and lends itself to auxiliary-field quantum Monte Carlo methods[96,97]. We perform finite-temperature simulations in the grand canonical ensemble and tune the chemical potential $\mu(T)$ to half fill the A_{1c} band. We consider a range of Hubbard interactions $|U|$ smaller than the single-particle gap $|t|$ above the A_{1c} band: $|U| = 3, 4, 5$, with $|t| = 6$. These parameters set us away from the isolated flat band regime $|U| \ll |t|$. We focus on a system with 6×6 unit cells and periodic boundary conditions.

We can directly extract the finite-temperature superfluid weight $D_s(T)$ from the Monte Carlo results[60]. The transition temperature T_c is determined by the Nelson-Kosterlitz criterion[62]: $T_c = \pi D_s^-/2$, where D_s^- is the superfluid weight at the critical temperature approached from below. In Fig. 3, we plot $D_s(T)$ for different $|U|$ as a function of $T/|U|$, finding the curves collapse on top of each other. This confirms $T_c \propto |U|$[100]. Our results prove that a coherent superconductor emerges upon inclusion of an attractive Hubbard interaction in the OWC flat bands, as in topological bands[26,100,101]. Ref. 26 discusses the contrasting case of trivial atomic bands.

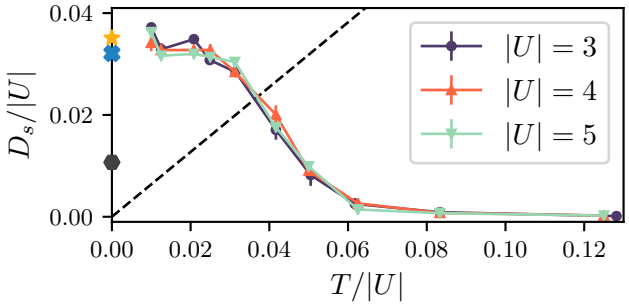

FIG. 3. Monte Carlo. The superfluid weight D_s as a function of temperature T is computed from Monte Carlo simulations on H in Eq. (23)[98,99]. We consider $|U| = 3, 4, 5$ with $|t| = 6$ in a system with 6×6 unit cells. The crossing of D_s with the dashed line $2T/\pi$ indicates the Berezinskii-Kosterlitz-Thouless superconducting transition. The yellow star/ blue cross indicate the mean-field $D_s(T = 0)$ obtained from a multi-band/ isolated flat band calculation (Eq. (10)). The gray hexagon shows the RSI bound on $D_s(T = 0)$.

We can compare the results of our Monte Carlo simulations to the zero temperature predictions of BCS theory. In particular, we recall in Ref. 60 that the BCS wavefunction is an exact zero-temperature ground state of the attractive Hubbard model projected into the flat bands[51], as follows from the equal weight of the flat band's Wannier function over all orbitals in the unit cell[42]. The blue cross in Fig. 3 shows the result of the analytical mean-field calculation after projection into the flat band. Alternatively, we solve the multi-band mean-field theory numerically in Ref. 60. The result is shown with the yellow star in Fig. 3. The agreement between our finite-temperature Monte Carlo simulations and the zero temperature mean-field calculations justify the use of the BCS result in Eq. (1), showing that our lower bounds successfully describe the many-body physics.

Discussion. We have shown that the RSIs characterizing the quantum geometry have a profound influence on the interacting groundstate when the flat bands are partially filled. Our lower bound for the superfluid weight is nontrivial in OWCs where the Wannier charge centers are obstructed from the atoms. Our bounds are not saturated by the Hamiltonian in Eq. (7), but we hope that future work can improve these bounds to be tight. Our RSI bounds also apply to OWCs with corner states, as well as stable and fragile topological phases[102,103]. Conceptually, the gauge-invariant expression Eq. (14) in terms of the correlation function shows that long-ranged Wannier functions are *not* essential to the lower bound. Any Wannier function which is supported over multiple unit cells[44,57], as can be enforced by symmetry in a OWC state, produces a quantized RSI lower bound. Our derivation is general for arbitrary bands and arbitrary symmetries. Although we studied the problem in 2D, our method is generalizable to 3D where flat band OWCs have been exhaustively identified[56].

ACKNOWLEDGMENTS

J.H-A. thanks Zhi-Da Song and Dylan King for useful discussions, and gratefully acknowledges insight Päivi Törmä. J.H-A. is supported by a Marshall Scholarship funded by the Marshall Aid Commemoration Commission. V.P., and S.D.H. acknowledge support from the Swiss National Science Foundation, the NCCR QSIT, the Swiss National Supercomputing Centre (CSCS) under project ID eth5b, and the European Research Council under the Grant Agreement No. 771503 (TopMechMat). F.S. was supported by a fellowship at the Princeton Center for Theoretical Science. B.A.B thanks funding from the European Research Council under the Grant Agreement no. 101020833 (SuperFlat). B.A.B. was also supported by the U.S. Department of Energy (Grant No. DE-SC0016239) and was partially supported by the National Science Foundation (EAGER Grant No. DMR 1643312), a Simons Investigator grant (No. 404513), the Office of Naval Research (ONR Grant No. N00014-20-1-2303), the Packard Foundation, the Schmidt Fund for Innovative Research, the BSF Israel US foundation (Grant No. 2018226), the Gordon and Betty Moore Foundation through Grant No. GBMF8685 towards the Princeton theory program, a Guggenheim Fellowship from the John Simon Guggenheim Memorial Foundation, and the NSF-MRSEC (Grant No. DMR2011750). The auxiliary-field QMC simulations were carried out with the ALF package available at https://git.physik.uni-wuerzburg.de/ALF/ALF.

[1] Christian Brouder, Gianluca Panati, Matteo Calandra, Christophe Mourougane, and Nicola Marzari. Exponential localization of wannier functions in insulators. *Physical Review Letters*, 98(4), Jan 2007. ISSN 1079-7114. doi:10.1103/physrevlett.98.046402.

[2] D J Thouless. Wannier functions for magnetic sub-bands. *Journal of Physics C: Solid State Physics*, 17(12):L325–L327, apr 1984. doi:10.1088/0022-3719/17/12/003. URL `https://doi.org/10.1088/0022-3719/17/12/003`.

[3] Domenico Monaco, Gianluca Panati, Adriano Pisante, and Stefan Teufel. Optimal Decay of Wannier functions in Chern and Quantum Hall Insulators. *Communications in Mathematical Physics*, January 2018. doi:10.1007/s00220-017-3067-7.

[4] Nicola Marzari, Arash A. Mostofi, Jonathan R. Yates, Ivo Souza, and David Vanderbilt. Maximally localized Wannier functions: Theory and applications. *Reviews of Modern Physics*, 84(4):1419–1475, October 2012. doi: 10.1103/RevModPhys.84.1419.

[5] Jennifer Cano and Barry Bradlyn. Band Representations and Topological Quantum Chemistry. *arXiv e-prints*, art. arXiv:2006.04890, June 2020.

[6] Barry Bradlyn, L. Elcoro, Jennifer Cano, M. G. Vergniory, Zhijun Wang, C. Felser, M. I. Aroyo, and B. Andrei Bernevig. Topological quantum chemistry. *Nature (London)*, 547(7663):298–305, Jul 2017. doi: 10.1038/nature23268.

[7] Zhida Song, L. Elcoro, Nicolas Regnault, and B. Andrei Bernevig. Fragile Phases As Affine Monoids: Classification and Material Examples. *arXiv e-prints*, art. arXiv:1905.03262, May 2019.

[8] Hoi Chun Po, Ashvin Vishwanath, and Haruki Watanabe. Complete theory of symmetry-based indicators of band topology. *Nature Communications*, 8:50, June 2017. doi: 10.1038/s41467-017-00133-2.

[9] Jorrit Kruthoff, Jan de Boer, Jasper van Wezel, Charles L. Kane, and Robert-Jan Slager. Topological classification of crystalline insulators through band structure combinatorics. *Phys. Rev. X*, 7:041069, Dec 2017. doi: 10.1103/PhysRevX.7.041069. URL `https://link.aps.org/doi/10.1103/PhysRevX.7.041069`.

[10] Hoi Chun Po, Haruki Watanabe, and Ashvin Vishwanath. Fragile Topology and Wannier Obstructions. *Phys. Rev. Lett.*, 121(12):126402, September 2018. doi: 10.1103/PhysRevLett.121.126402.

[11] Barry Bradlyn, Zhijun Wang, Jennifer Cano, and B. Andrei Bernevig. Disconnected elementary band representations, fragile topology, and wilson loops as topological indices: An example on the triangular lattice. *Physical Review B*, 99(4), Jan 2019. ISSN 2469-9969. doi: 10.1103/physrevb.99.045140. URL `http://dx.doi.org/10.1103/PhysRevB.99.045140`.

[12] Adrien Bouhon, Annica M. Black-Schaffer, and Robert-Jan Slager. Wilson loop approach to fragile topology of split elementary band representations and topological crystalline insulators with time-reversal symmetry. *Phys. Rev. B*, 100(19):195135, November 2019. doi: 10.1103/PhysRevB.100.195135.

[13] Eslam Khalaf, Hoi Chun Po, Ashvin Vishwanath, and Haruki Watanabe. Symmetry Indicators and Anomalous Surface States of Topological Crystalline Insulators. *Physical Review X*, 8(3):031070, July 2018. doi: 10.1103/PhysRevX.8.031070.

[14] M. Z. Hasan and C. L. Kane. Colloquium: Topological insulators. *Reviews of Modern Physics*, 82(4):3045–3067, October 2010. doi:10.1103/RevModPhys.82.3045.

[15] Zhi-Da Song, Luis Elcoro, and B. Andrei Bernevig. Twisted bulk-boundary correspondence of fragile topology. *Science*, 367(6479):794–797, February 2020. doi: 10.1126/science.aaz7650.

[16] Valerio Peri, Zhi-Da Song, Marc Serra-Garcia, Pascal Engeler, Raquel Queiroz, Xueqin Huang, Weiyin Deng, Zhengyou Liu, B. Andrei Bernevig, and Sebastian D. Huber. Experimental characterization of fragile topology in an acoustic metamaterial. *Science*, 367(6479):797–800, 2020. ISSN 0036-8075. doi:10.1126/science.aaz7654. URL `https://science.sciencemag.org/content/367/6479/797`.

[17] Jonah Herzog-Arbeitman, Zhi-Da Song, Nicolas Regnault, and B. Andrei Bernevig. Hofstadter topology: Noncrystalline topological materials at high flux. *Phys. Rev. Lett.*, 125:236804, Dec 2020. doi: 10.1103/PhysRevLett.125.236804. URL `https://link.aps.org/doi/10.1103/PhysRevLett.125.236804`.

[18] Shang Liu, Ashvin Vishwanath, and Eslam Khalaf. Shift insulators: Rotation-protected two-dimensional topolog-

ical crystalline insulators. *Phys. Rev. X*, 9:031003, Jul 2019. doi:10.1103/PhysRevX.9.031003. URL https://link.aps.org/doi/10.1103/PhysRevX.9.031003.

[19] Maia G. Vergniory, Benjamin J. Wieder, Luis Elcoro, Stuart S. P. Parkin, Claudia Felser, B. Andrei Bernevig, and Nicolas Regnault. All Topological Bands of All Stoichiometric Materials. *arXiv e-prints*, art. arXiv:2105.09954, May 2021.

[20] Luis Elcoro, Zhida Song, and B. Andrei Bernevig. Application of induction procedure and Smith decomposition in calculation and topological classification of electronic band structures in the 230 space groups. *Phys. Rev. B*, 102(3):035110, July 2020. doi:10.1103/PhysRevB.102.035110.

[21] Jennifer Cano, L. Elcoro, M. I. Aroyo, B. Andrei Bernevig, and Barry Bradlyn. Topology invisible to eigenvalues in obstructed atomic insulators. *arXiv e-prints*, art. arXiv:2107.00647, July 2021.

[22] Luis Elcoro, Benjamin J. Wieder, Zhida Song, Yuanfeng Xu, Barry Bradlyn, and B. Andrei Bernevig. Magnetic Topological Quantum Chemistry. *arXiv e-prints*, art. arXiv:2010.00598, October 2020.

[23] Sebastiano Peotta and Päivi Törmä. Superfluidity in topologically nontrivial flat bands. *Nature Communications*, 6:8944, November 2015. doi:10.1038/ncomms9944.

[24] P. Törmä, S. Peotta, and B. A. Bernevig. Superfluidity and Quantum Geometry in Twisted Multilayer Systems. *arXiv e-prints*, art. arXiv:2111.00807, November 2021.

[25] Zhi-Da Song, Zhijun Wang, Wujun Shi, Gang Li, Chen Fang, and B. Andrei Bernevig. All Magic Angles in Twisted Bilayer Graphene are Topological. *Phys. Rev. Lett.*, 123(3):036401, Jul 2019. doi:10.1103/PhysRevLett.123.036401.

[26] Valerio Peri, Zhi-Da Song, B. Andrei Bernevig, and Sebastian D. Huber. Fragile Topology and Flat-Band Superconductivity in the Strong-Coupling Regime. *Phys. Rev. Lett.*, 126(2):027002, January 2021. doi:10.1103/PhysRevLett.126.027002.

[27] Cyprian Lewandowski, Stevan Nadj-Perge, and Debanjan Chowdhury. Does filling-dependent band renormalization aid pairing in twisted bilayer graphene? *npj Quantum Materials*, 6:82, January 2021. doi:10.1038/s41535-021-00379-6.

[28] Zhi-Da Song, Biao Lian, Nicolas Regnault, and B. Andrei Bernevig. Twisted bilayer graphene. II. Stable symmetry anomaly. *Phys. Rev. B*, 103(20):205412, May 2021. doi:10.1103/PhysRevB.103.205412.

[29] A. Julku, T. J. Peltonen, L. Liang, T. T. Heikkilä, and P. Törmä. Superfluid weight and Berezinskii-Kosterlitz-Thouless transition temperature of twisted bilayer graphene. *Phys. Rev. B*, 101(6):060505, February 2020. doi:10.1103/PhysRevB.101.060505.

[30] Liujun Zou, Hoi Chun Po, Ashvin Vishwanath, and T. Senthil. Band structure of twisted bilayer graphene: Emergent symmetries, commensurate approximants, and wannier obstructions. *Phys. Rev. B*, 98:085435, Aug 2018. doi:10.1103/PhysRevB.98.085435. URL https://link.aps.org/doi/10.1103/PhysRevB.98.085435.

[31] Swati Chaudhary, Cyprian Lewandowski, and Gil Refael. Shift-current response as a probe of quantum geometry and electron-electron interactions in twisted bilayer graphene. *arXiv e-prints*, art. arXiv:2107.09090, July 2021.

[32] Aaron Chew, Yijie Wang, B. Andrei Bernevig, and Zhi-Da Song. Higher-Order Topological Superconductivity in Twisted Bilayer Graphene. *arXiv e-prints*, art. arXiv:2108.05373, August 2021.

[33] Frank Schindler, Barry Bradlyn, Mark H. Fischer, and Titus Neupert. Pairing Obstructions in Topological Superconductors. *Phys. Rev. Lett.*, 124(24):247001, June 2020. doi:10.1103/PhysRevLett.124.247001.

[34] Jianpeng Liu, Junwei Liu, and Xi Dai. Pseudo landau level representation of twisted bilayer graphene: Band topology and implications on the correlated insulating phase. *Phys. Rev. B*, 99:155415, Apr 2019. doi:10.1103/PhysRevB.99.155415. URL https://link.aps.org/doi/10.1103/PhysRevB.99.155415.

[35] Yuan Cao, V. Fatemi, S. Fang, K. Watanabe, T. Taniguchi, E. Kaxiras, and P. Jarillo-Herrero. Unconventional superconductivity in magic-angle graphene superlattices. *Nature*, 556:43–50, 2018.

[36] Rafi Bistritzer and Allan H. MacDonald. Moiré bands in twisted double-layer graphene. *Proceedings of the National Academy of Science*, 108(30):12233–12237, Jul 2011. doi:10.1073/pnas.1108174108.

[37] Petr Stepanov, Ming Xie, Takashi Taniguchi, Kenji Watanabe, Xiaobo Lu, Allan H. MacDonald, B. Andrei Bernevig, and Dmitri K. Efetov. Competing zero-field Chern insulators in Superconducting Twisted Bilayer Graphene. *arXiv e-prints*, art. arXiv:2012.15126, December 2020.

[38] Yonglong Xie, Biao Lian, Berthold Jäck, Xiaomeng Liu, Cheng-Li Chiu, Kenji Watanabe, Takashi Taniguchi, B. Andrei Bernevig, and Ali Yazdani. Spectroscopic signatures of many-body correlations in magic-angle twisted bilayer graphene. *Nature (London)*, 572(7767):101–105, Jul 2019. doi:10.1038/s41586-019-1422-x.

[39] Yuan Cao, Valla Fatemi, Ahmet Demir, Shiang Fang, Spencer L. Tomarken, Jason Y. Luo, Javier D. Sanchez-Yamagishi, Kenji Watanabe, Takashi Taniguchi, Efthimios Kaxiras, Ray C. Ashoori, and Pablo Jarillo-Herrero. Correlated insulator behaviour at half-filling in magic-angle graphene superlattices. *Nature (London)*, 556 (7699):80–84, Apr 2018. doi:10.1038/nature26154.

[40] Eva Y. Andrei, Dmitri K. Efetov, Pablo Jarillo-Herrero, Allan H. MacDonald, Kin Fai Mak, T. Senthil, Emanuel Tutuc, Ali Yazdani, and Andrea F. Young. The marvels of moiré materials. *Nature Reviews Materials*, 6(3):201–206, March 2021. ISSN 2058-8437. doi:10.1038/s41578-021-00284-1.

[41] Haidong Tian, Shi Che, Tianyi Xu, Patrick Cheung, Kenji Watanabe, Takashi Taniguchi, Mohit Randeria, Fan Zhang, Chun Ning Lau, and Marc W. Bockrath. Evidence for Flat Band Dirac Superconductor Originating from Quantum Geometry. *arXiv e-prints*, art. arXiv:2112.13401, December 2021.

[42] Aleksi Julku, Sebastiano Peotta, Tuomas I. Vanhala, Dong-Hee Kim, and Päivi Törmä. Geometric Origin of Superfluidity in the Lieb-Lattice Flat Band. *Phys. Rev. Lett.*, 117(4):045303, July 2016. doi:10.1103/PhysRevLett.117.045303.

[43] Tamaghna Hazra, Nishchhal Verma, and Mohit Randeria. Bounds on the superconducting transition temperature: Applications to twisted bilayer graphene and cold atoms. *Phys. Rev. X*, 9:031049, Sep 2019. doi:10.1103/PhysRevX.9.031049. URL https://link.aps.org/doi/10.1103/PhysRevX.9.031049.

[44] Murad Tovmasyan, Sebastiano Peotta, Long Liang, Päivi Törmä, and Sebastian D. Huber. Preformed pairs in flat Bloch bands. *Phys. Rev. B*, 98(13):134513, October 2018. doi:10.1103/PhysRevB.98.134513.

[45] Johannes S. Hofmann, Debanjan Chowdhury, Steven A. Kivelson, and Erez Berg. Superconductivity is boundless. *arXiv e-prints*, art. arXiv:2105.09322, May 2021.

[46] Xiang Hu, Timo Hyart, Dmitry I. Pikulin, and Enrico Rossi. Geometric and conventional contribution to the superfluid weight in twisted bilayer graphene. *Phys. Rev. Lett.*, 123:237002, Dec 2019. doi: 10.1103/PhysRevLett.123.237002. URL `https://link.aps.org/doi/10.1103/PhysRevLett.123.237002`.

[47] P. Törmä, L. Liang, and S. Peotta. Quantum metric and effective mass of a two-body bound state in a flat band. *Phys. Rev. B*, 98(22):220511, December 2018. doi: 10.1103/PhysRevB.98.220511.

[48] Zhiqiang Wang, Gaurav Chaudhary, Qijin Chen, and K. Levin. Quantum geometric contributions to the bkt transition: Beyond mean field theory. *Phys. Rev. B*, 102:184504, Nov 2020. doi: 10.1103/PhysRevB.102.184504. URL `https://link.aps.org/doi/10.1103/PhysRevB.102.184504`.

[49] Nishchhal Verma, Tamaghna Hazra, and Mohit Randeria. Optical spectral weight, phase stiffness, and Tc bounds for trivial and topological flat band superconductors. *Proceedings of the National Academy of Science*, 118(34): 2106744118, August 2021. doi:10.1073/pnas.2106744118.

[50] Fang Xie, Zhida Song, Biao Lian, and B. Andrei Bernevig. Topology-bounded superfluid weight in twisted bilayer graphene. *Phys. Rev. Lett.*, 124:167002, Apr 2020. doi: 10.1103/PhysRevLett.124.167002. URL `https://link.aps.org/doi/10.1103/PhysRevLett.124.167002`.

[51] Murad Tovmasyan, Sebastiano Peotta, Päivi Törmä, and Sebastian D. Huber. Effective theory and emergent SU(2) symmetry in the flat bands of attractive hubbard models. *Phys. Rev. B*, 94:245149, Dec 2016. doi: 10.1103/PhysRevB.94.245149. URL `https://link.aps.org/doi/10.1103/PhysRevB.94.245149`.

[52] Dumitru Călugăru, Aaron Chew, Luis Elcoro, Nicolas Regnault, Zhi-Da Song, and B. Andrei Bernevig. General Construction and Topological Classification of All Magnetic and Non-Magnetic Flat Bands. *arXiv e-prints*, art. arXiv:2106.05272, June 2021.

[53] Benjamin J. Wieder, Barry Bradlyn, Jennifer Cano, Zhijun Wang, Maia G. Vergniory, Luis Elcoro, Alexey A. Soluyanov, Claudia Felser, Titus Neupert, Nicolas Regnault, and B. Andrei Bernevig. Topological Materials Discovery from Nonmagnetic Crystal Symmetry. *arXiv e-prints*, art. arXiv:2106.00709, June 2021.

[54] Yuanfeng Xu, Luis Elcoro, Zhi-Da Song, Benjamin J. Wieder, M. G. Vergniory, Nicolas Regnault, Yulin Chen, Claudia Felser, and B. Andrei Bernevig. High-throughput calculations of magnetic topological materials. *Nature (London)*, 586(7831):702–707, October 2020. doi: 10.1038/s41586-020-2837-0.

[55] Yuanfeng Xu, Luis Elcoro, Zhi-Da Song, M. G. Vergniory, Claudia Felser, Stuart S. P. Parkin, Nicolas Regnault, Juan L. Mañes, and B. Andrei Bernevig. Filling-Enforced Obstructed Atomic Insulators. *arXiv e-prints*, art. arXiv:2106.10276, June 2021.

[56] Nicolas Regnault, Yuanfeng Xu, Ming-Rui Li, Da-Shuai Ma, Milena Jovanovic, Ali Yazdani, Stuart S. P. Parkin, Claudia Felser, Leslie M. Schoop, N. Phuan Ong, Robert J. Cava, Luis Elcoro, Zhi-Da Song, and B. Andrei Bernevig. Catalogue of Flat Band Stoichiometric Materials. *arXiv e-prints*, art. arXiv:2106.05287, June 2021.

[57] Frank Schindler and B. Andrei Bernevig. Non-Compact Atomic Insulators. *arXiv e-prints*, art. arXiv:2107.13556, July 2021.

[58] Frédéric Piéchon, Arnaud Raoux, Jean-Noël Fuchs, and Gilles Montambaux. Geometric orbital susceptibility: Quantum metric without berry curvature. *Phys. Rev. B*, 94:134423, Oct 2016. doi: 10.1103/PhysRevB.94.134423. URL `https://link.aps.org/doi/10.1103/PhysRevB.94.134423`.

[59] Long Liang, Tuomas I Vanhala, Sebastiano Peotta, Topi Siro, Ari Harju, and Päivi Törmä. Band geometry, berry curvature, and superfluid weight. *Physical Review B*, 95 (2):024515, 2017.

[60] See supplementary materials for a description of additional calculations.

[61] J. Kosterlitz and D. Thouless. Ordering, metastability and phase transitions in two-dimensional systems. *Journal of Physics C: Solid State Physics*, 6:1181–1203, 1973.

[62] David R. Nelson and J. M. Kosterlitz. Universal jump in the superfluid density of two-dimensional superfluids. *Phys. Rev. Lett.*, 39:1201–1205, Nov 1977. doi: 10.1103/PhysRevLett.39.1201. URL `https://link.aps.org/doi/10.1103/PhysRevLett.39.1201`.

[63] R. Resta. The insulating state of matter: a geometrical theory. *European Physical Journal B*, 79(2):121–137, January 2011. doi:10.1140/epjb/e2010-10874-4.

[64] Johannes Mitscherling and Tobias Holder. Bound on resistivity in flat band materials due to the quantum metric. *arXiv e-prints*, art. arXiv:2110.14658, October 2021.

[65] Tyler B. Smith, Lakshmi Pullasseri, and Ajit Srivastava. Momentum-space Gravity from the Quantum Geometry and Entropy of Bloch Electrons. *arXiv e-prints*, art. arXiv:2108.02216, August 2021.

[66] Aleksi Julku, Georg M. Bruun, and Päivi Törmä. Quantum geometry and flat band bose-einstein condensation. *Phys. Rev. Lett.*, 127:170404, Oct 2021. doi: 10.1103/PhysRevLett.127.170404. URL `https://link.aps.org/doi/10.1103/PhysRevLett.127.170404`.

[67] Ran Cheng. Quantum Geometric Tensor (Fubini-Study Metric) in Simple Quantum System: A pedagogical Introduction. *arXiv e-prints*, art. arXiv:1012.1337, December 2010.

[68] Bruno Mera, Anwei Zhang, and Nathan Goldman. Relating the topology of Dirac Hamiltonians to quantum geometry: When the quantum metric dictates Chern numbers and winding numbers. *arXiv e-prints*, art. arXiv:2106.00800, June 2021.

[69] Enrico Rossi. Quantum Metric and Correlated States in Two-dimensional Systems. *arXiv e-prints*, art. arXiv:2108.11478, August 2021.

[70] Fengcheng Wu and S. Das Sarma. Quantum geometry and stability of moiré flatband ferromagnetism. *Phys. Rev. B*, 102:165118, Oct 2020. doi: 10.1103/PhysRevB.102.165118. URL `https://link.aps.org/doi/10.1103/PhysRevB.102.165118`.

[71] Kristian Hauser A. Villegas and Bo Yang. Anomalous Higgs oscillations mediated by Berry curvature and quantum metric. *arXiv e-prints*, art. arXiv:2010.07751, October 2020.

[72] Jie Wang, Jennifer Cano, Andrew J. Millis, Zhao Liu, and Bo Yang. Exact Landau Level Description of Geom-

etry and Interaction in a Flatband. *arXiv e-prints*, art. arXiv:2105.07491, May 2021.

[73] Titus Neupert, Claudio Chamon, and Christopher Mudry. Measuring the quantum geometry of bloch bands with current noise. *Phys. Rev. B*, 87:245103, Jun 2013. doi: 10.1103/PhysRevB.87.245103. URL https://link.aps.org/doi/10.1103/PhysRevB.87.245103.

[74] M. Iskin. Two-body problem in a multiband lattice and the role of quantum geometry. *Phys. Rev. A*, 103: 053311, May 2021. doi:10.1103/PhysRevA.103.053311. URL https://link.aps.org/doi/10.1103/PhysRevA.103.053311.

[75] Inti Sodemann and Liang Fu. Quantum Nonlinear Hall Effect Induced by Berry Curvature Dipole in Time-Reversal Invariant Materials. *Phys. Rev. Lett.*, 115(21):216806, November 2015. doi:10.1103/PhysRevLett.115.216806.

[76] Long Liang, Sebastiano Peotta, Ari Harju, and Päivi Törmä. Wave-packet dynamics of Bogoliubov quasiparticles: Quantum metric effects. *Phys. Rev. B*, 96(6):064511, August 2017. doi:10.1103/PhysRevB.96.064511.

[77] Qiong Ma, Adolfo G Grushin, and Kenneth S Burch. Topology and geometry under the nonlinear electromagnetic spotlight. *Nature Materials*, pages 1–14, 2021.

[78] Gabriel E. Topp, Christian J. Eckhardt, Dante M. Kennes, Michael A. Sentef, and Päivi Törmä. Light-matter coupling and quantum geometry in moiré materials. *Phys. Rev. B*, 104:064306, Aug 2021. doi: 10.1103/PhysRevB.104.064306. URL https://link.aps.org/doi/10.1103/PhysRevB.104.064306.

[79] Junyeong Ahn, Guang-Yu Guo, Naoto Nagaosa, and Ashvin Vishwanath. Riemannian Geometry of Resonant Optical Responses. *arXiv e-prints*, art. arXiv:2103.01241, March 2021.

[80] Yang Gao, Shengyuan A. Yang, and Qian Niu. Field Induced Positional Shift of Bloch Electrons and Its Dynamical Implications. *Phys. Rev. Lett.*, 112(16):166601, April 2014. doi:10.1103/PhysRevLett.112.166601.

[81] J Orenstein, JE Moore, T Morimoto, DH Torchinsky, JW Harter, and D Hsieh. Topology and symmetry of quantum materials via nonlinear optical responses. *Annual Review of Condensed Matter Physics*, 12:247–272, 2021.

[82] Nitesh Kumar, Satya N Guin, Kaustuv Manna, Chandra Shekhar, and Claudia Felser. Topological quantum materials from the viewpoint of chemistry. *Chemical Reviews*, 121(5):2780–2815, 2020.

[83] J. Anandan and Y. Aharonov. Geometry of quantum evolution. *Phys. Rev. Lett.*, 65:1697–1700, Oct 1990. doi: 10.1103/PhysRevLett.65.1697. URL https://link.aps.org/doi/10.1103/PhysRevLett.65.1697.

[84] Note that the off-diagonal g_{12} term do not appear in the trace, but this term is only relevant in highly anisotropic systems.

[85] Jennifer Cano, Barry Bradlyn, Zhijun Wang, L. Elcoro, M. G. Vergniory, C. Felser, M. I. Aroyo, and B. Andrei Bernevig. Building blocks of topological quantum chemistry: Elementary band representations. *Phys. Rev. B*, 97 (3):035139, Jan 2018. doi:10.1103/PhysRevB.97.035139.

[86] J. Zak. Band representations and symmetry types of bands in solids. *Phys. Rev. B*, 23:2824–2835, Mar 1981. doi:10.1103/PhysRevB.23.2824. URL https://link.aps.org/doi/10.1103/PhysRevB.23.2824.

[87] MI Aroyo, JM Perez-Mato, Cesar Capillas, Eli Kroumova, Svetoslav Ivantchev, Gotzon Madariaga, Asen Kirov, and Hans Wondratschek. Bilbao crystallographic server: I. databases and crystallographic computing programs. *ZEITSCHRIFT FUR KRISTALLOGRAPHIE*, 221:15–27, 01 2006. doi:10.1524/zkri.2006.221.1.15.

[88] Mois I. Aroyo, Asen Kirov, Cesar Capillas, J. M. Perez-Mato, and Hans Wondratschek. Bilbao Crystallographic Server. II. Representations of crystallographic point groups and space groups. *Acta Crystallographica Section A*, 62(2):115–128, Mar 2006. doi: 10.1107/S0108767305040286.

[89] M. G. Vergniory, L. Elcoro, Zhijun Wang, Jennifer Cano, C. Felser, M. I. Aroyo, B. Andrei Bernevig, and Barry Bradlyn. Graph theory data for topological quantum chemistry. *Phys. Rev. E*, 96:023310, Aug 2017. doi: 10.1103/PhysRevE.96.023310.

[90] A. Alexandradinata, Xi Dai, and B. Andrei Bernevig. Wilson-Loop Characterization of Inversion-Symmetric Topological Insulators. *Phys. Rev.*, B89(15):155114, 2014. doi:10.1103/PhysRevB.89.155114.

[91] W. P. Su, J. R. Schrieffer, and A. J. Heeger. Solitons in polyacetylene. *Phys. Rev. Lett.*, 42:1698–1701, Jun 1979. doi:10.1103/PhysRevLett.42.1698. URL https://link.aps.org/doi/10.1103/PhysRevLett.42.1698.

[92] Titus Neupert and Frank Schindler. Lecture Notes on Topological Crystalline Insulators. *arXiv e-prints*, art. arXiv:1810.03484, October 2018.

[93] Frank Schindler. Dirac equation perspective on higher-order topological insulators. *Journal of Applied Physics*, 128(22):221102, December 2020. doi:10.1063/5.0035850.

[94] B. Andrei Bernevig and Taylor L. Hughes. *Topological Insulators and Topological Superconductors.* Princeton University Press, student edition edition, 2013. ISBN 9780691151755.

[95] Henry Wolkowicz and George PH Styan. Bounds for eigenvalues using traces. *Linear algebra and its applications*, 29:471–506, 1980.

[96] R. Blankenbecler, D. J. Scalapino, and R. L. Sugar. Monte carlo calculations of coupled boson-fermion systems. i. *Phys. Rev. D*, 24:2278–2286, Oct 1981. doi: 10.1103/PhysRevD.24.2278. URL https://link.aps.org/doi/10.1103/PhysRevD.24.2278.

[97] Martin Bercx, Florian Goth, Johannes S. Hofmann, and Fakher F. Assaad. The ALF (Algorithms for Lattice Fermions) project release 1.0. Documentation for the auxiliary field quantum Monte Carlo code. *SciPost Phys.*, 3:013, 2017. doi:10.21468/SciPostPhys.3.2.013. URL https://scipost.org/10.21468/SciPostPhys.3.2.013.

[98] D. J. Scalapino, S. R. White, and S. C. Zhang. Superfluid density and the drude weight of the hubbard model. *Phys. Rev. Lett.*, 68:2830–2833, May 1992. doi: 10.1103/PhysRevLett.68.2830. URL https://link.aps.org/doi/10.1103/PhysRevLett.68.2830.

[99] Douglas J. Scalapino, Steven R. White, and Shoucheng Zhang. Insulator, metal, or superconductor: The criteria. *Phys. Rev. B*, 47:7995–8007, Apr 1993. doi: 10.1103/PhysRevB.47.7995. URL https://link.aps.org/doi/10.1103/PhysRevB.47.7995.

[100] Johannes S. Hofmann, Erez Berg, and Debanjan Chowdhury. Superconductivity, pseudogap, and phase separation in topological flat bands. *Phys. Rev. B*, 102:201112(R), Nov 2020. doi: 10.1103/PhysRevB.102.201112. URL https://link.aps.org/doi/10.1103/PhysRevB.102.201112.

[101] Johannes S. Hofmann, Erez Berg, and Debanjan Chowdhury. Superconductivity, pseudogap, and phase separation in topological flat bands. *Phys. Rev. B*, 102(20):201112, November 2020. doi: 10.1103/PhysRevB.102.201112.

[102] Wladimir A. Benalcazar, B. Andrei Bernevig, and Taylor L. Hughes. Electric multipole moments, topological multipole moment pumping, and chiral hinge states in crystalline insulators. *Phys. Rev. B*, 96(24):245115, Dec 2017. doi:10.1103/PhysRevB.96.245115.

[103] Wladimir A. Benalcazar, B. Andrei Bernevig, and Taylor L. Hughes. Quantized electric multipole insulators. *Science*, 357(6346):61–66, Jul 2017. doi: 10.1126/science.aah6442.